Lemke *et al.*: Computer Assisted Radiology and Surgery 2001, June 27–30, Berlin (Germany) — ©Elsevier

Visualization of Human Coronary Arteries with Quantification Results from 3-D and 4-D Computational Hemodynamics based upon Virtual Endoscopy

Andreas Wahle,[a] Steven C. Mitchell,[a] Sharan D. Ramaswamy,[b] Krishnan B. Chandran,[b] Milan Sonka[a]

The University of Iowa, Departments of [a]Electrical & Computer Engineering, [b]Biomedical Engineering, Iowa City, IA 52242–1527, U.S.A. (http://www.engineering.uiowa.edu/~awahle)

Keywords: Cardiovascular Imaging, Virtual Endoscopy, Angioscopy, Coronary Atherosclerosis, Computational Hemodynamics, Multimodal Image Fusion, Intravascular Ultrasound, Biplane Angiography

1. INTRODUCTION

Intravascular ultrasound (IVUS) imaging is complementary to conventional selective x-ray angiography and is used for assessment of obstructive coronary artery disease [1]. Figure 1 shows an example for both modalities applied to the same vessel. By fusion of IVUS with biplane angiography, a geometrically correct 3-D model can be derived [1–3]. The 3-D model provides a good basis for assessment of hemodynamic consequences of coronary disease via shear stress calculations based upon computational fluid dynamics (CFD) [4, 5]. Previous studies of computational hemodynamics have implicated regions of flow reversal and separation, as well as relatively low wall shear stresses and oscillating shear stresses, as causes for initiation and growth of atherosclerotic plaques [6]. In coronary arteries, translation, bending, and twisting as the cardiac muscles contract and relax during a cardiac cycle has a substantial impact on the hemodynamics [7]. This implies that the CFD analysis has to consider 3-D geometry and morphology of the vessel as well as its cross-sectional changes and the overall vessel motion throughout the cardiac cycle. In this paper, we are presenting our work in progress based upon 4-D models (3-D plus time) reconstructed via fusion of IVUS and biplane x-ray angiography, along with the modeling and visualization of the 3-D and 4-D data.

2. METHODS

2.1 IVUS–Angiography Fusion

The fusion system has been described in detail elsewhere [1–3]. For the 4-D reconstruction of the vessel lumen, the acquired data are first sorted into n sets of images according to the heart phase as identified by the ECG signal [5]. For each phase, the angiograms are segmented for the path of the catheter and the vessel outline. These data are then used to reconstruct a 3-D model of the catheter path and the approximate shapes of the cross-sections using a well-established method developed and validated at the German Heart Institute of Berlin [8]. The IVUS data are

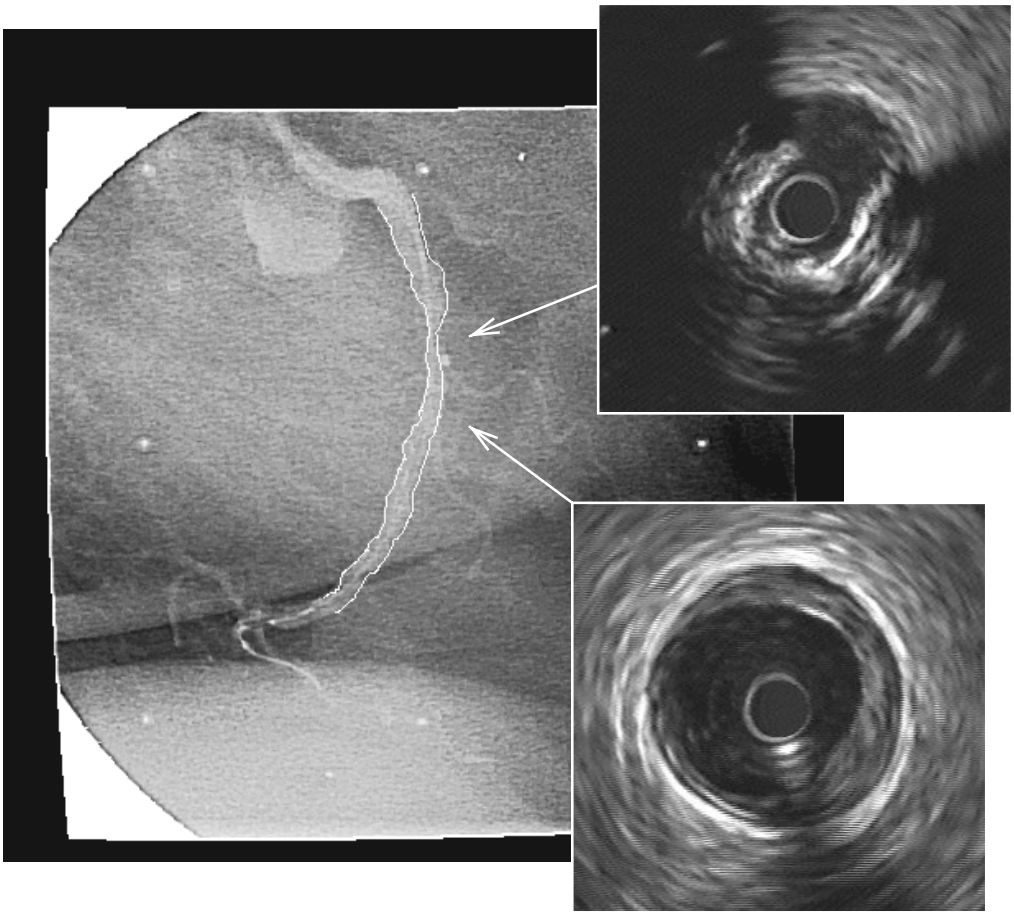

Figure 1: Angiogram of a stenosed right coronary artery in-vivo in 75° RAO projection with detected lumen contours inserted; the two IVUS frames were acquired within the stenosis (top) and about 10 mm distal of the stenosis (bottom) — calcifications as well as soft plaque are clearly depicted.

segmented for the lumen only, which is sufficient for the shear stress analysis. While the 4-D data set is created from the complete set of 3-D models, the fusion process is not performed entirely separately for each heart phase [5]. The regions-of-interest of one phase are used as initial guess for the next phase in IVUS segmentation, and the absolute orientation of the IVUS frame sets [2, 3] is calculated over all phases.

2.2 Computational Hemodynamics

For the CFD analysis on in-vivo vessels, the *U2RANS* software has been employed that was developed at the Iowa Institute of Hydraulic Research [9]. Alternatively, a commercial CFD package, *FLUENT* 5.3 (Fluent Inc., Lebanon NH, U.S.A.) was used. The *GRIDGEN* grid generation software (Pointwise Inc., Fort Worth TX, U.S.A.) was utilized to create meshes from the fusion results. In-vitro validation was performed in a computer simulation of a human aortic arc [5]. Up to now, CFD analysis is performed in 3-D only, considering steady-flow conditions in a structured grid; pulsatile non-steady flow and vessel motion will be approached soon after the 3-D methodology has been completely developed and validated. The vessel lumen surface is split and meshed into six independent domains that make up one volumetric 3-D mesh, which

is then used as input for the CFD system. As part of the geometry development, the grid density has been optimized based on a compromise between the grid size and the structural integrity of the mesh. An iterative procedure is performed to solve the equations of flow and space conservation. An initial pressure is assumed at the outlet boundary and subsequently adjusted based on a pressure-correction scheme, thus ensuring mass conservation [9].

2.3 Visualization

For presentation of the 3-D and 4-D data, the ISO-standardized *Virtual Reality Modeling Language* (VRML) is used, a platform-independent description language [3, 5, 10]. The lumen surface is triangulated and converted to an IndexedFaceSet, animation of the 4-D data is implemented using a CoordinateInterpolator node (Fig. 2). Aside the navigation using the standard controls of the VRML browser, an endoscopic mode has been introduced for virtual angioscopy. It features a comprehensive VRML external prototype library that includes *JavaScript* components [10]. The fly-through trajectory is determined automatically from catheter path or vessel centerline. The navigation within the vessel is performed through a control panel that is available on demand and can be hidden when not needed (Fig. 3). In all modes, the computed shear-stress data can be included by colorPerVertex encoding [5]. Furthermore, a mixed view of shear-stress values and original (raw) IVUS data can be chosen to visually correlate the CFD results with the actual images.

3. IN-VIVO STUDY

Figures 1–3 are part of a feasibility study performed on a single patient out of a total of seven patients undergoing routine intervention and stent placement. These in-vivo data have been acquired at the University of Iowa Hospitals and Clinics, the University Hospital Essen (Germany), and the Brigham and Women's Hospital at Harvard Medical School (Boston MA). In the patient shown here, a sheathed catheter with 30 MHz rotating transducer and 0.5 mm/s automated pullback was used. The acquired angiographic and IVUS data were split into six heart phases at 0%, 17%, 33%, 50%, 67%, and 83% of the R–R intervals according to the ECG signal [5]. The vessel segment under consideration was approximately 75 mm in length. The 720 vertex points per IVUS frame have been downsampled to 30 points per contour for visualization, and to 76 points for CFD analysis. Longitudinal smoothing was performed by moving average over 3–5 frames along the vessel. For each phase, CFD analysis was performed individually. 172 cross-sections à 76 vertex points were reconstructed per phase and downsampled in longitudinal direction to 150 cross-sections, thus resulting in six meshes with $20 \times 150 \times 20 = 60{,}000$ grid points each. Negative skewing and negative cells in the mesh were removed using a partial differential equation solver. Constant fluid property parameters for whole human blood were used based on a Reynold's number of 500; the density of blood was specified as $\rho = 1050\,\mathrm{kg/m^3}$ with a kinematic viscosity $\nu = 4 \cdot 10^{-6}\,\mathrm{m^2/s}$; for the inlet velocity boundary condition, a flat velocity profile under steady-state conditions was used (mean flow rate $\overline{Q} = 3.376 \cdot 10^{-6}\,\mathrm{m^3/s}$). These values were slightly adjusted from our previous study [5], to be in accordance with widely accepted constants [11, 12]. Blood was treated as an incompressible, homogenous, and Newtonian fluid. Further, the no-slip boundary condition was assumed at the vessel wall and a constant pressure outlet condition was utilized in the CFD model [5].

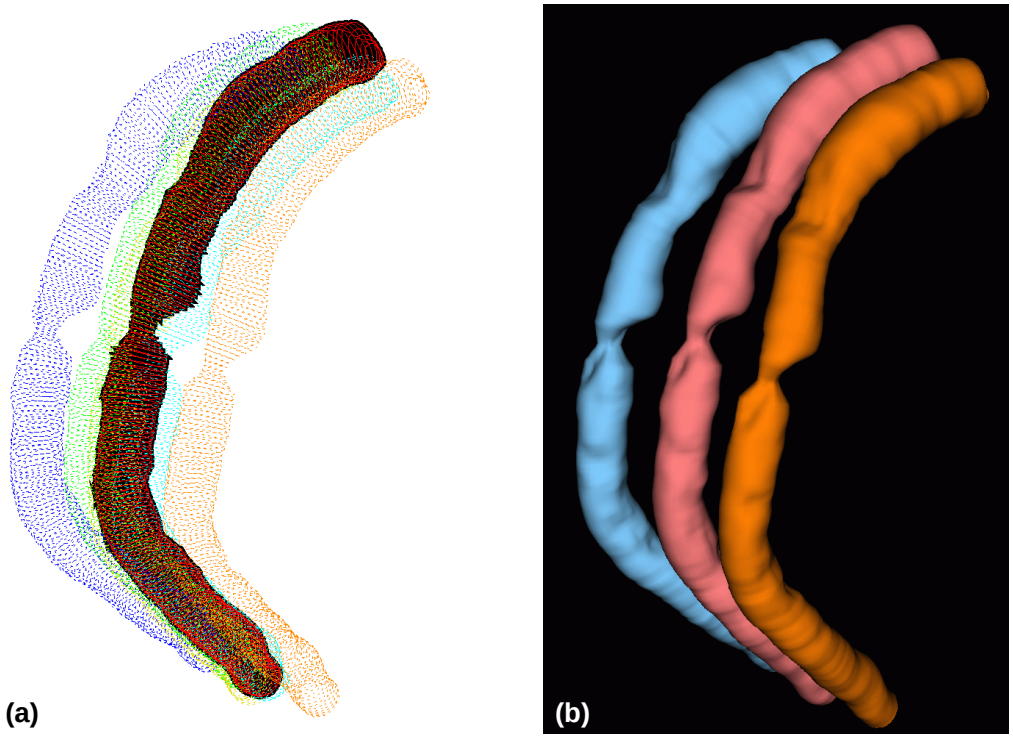

Figure 2: Reconstructed 4-D model of the vessel lumen resulting from the fusion process in anterior view; (a) the six phases as wire frames with the end-diastolic phase emphasized, (b) VRML surface representation of the end-diastolic phase as well as phases representing the maximum excursion.

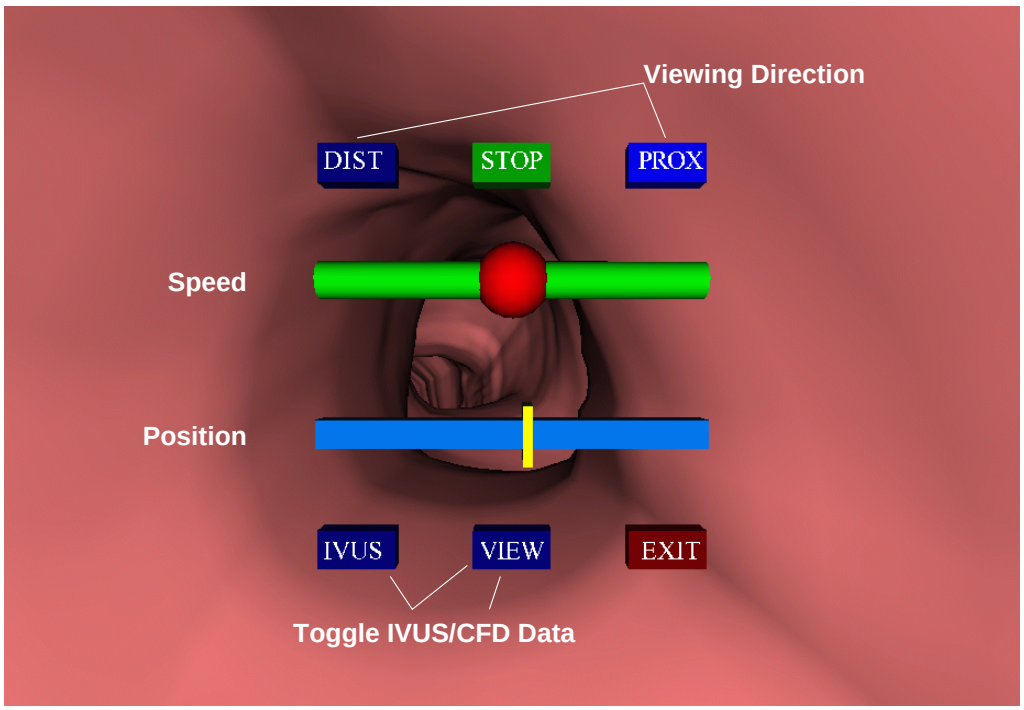

Figure 3: Endoscopic scene using our VRML prototype library with (labeled) control panel inserted; viewpoint is distal of the stenosis, looking against the direction of the blood flow.

4. RESULTS

Figure 2(a) shows the six reconstructed phases as wire-frame models in a resolution of 172 cross sections with 30 vertex points each. After triangulation, approximately 1.8 MB of VRML code was generated automatically. Animation could be achieved in real-time, Fig. 2(b) shows how the vessel is moving from the end-diastolic phase first to its maximum-distance location from the heart long axis before contracting in the systole. The endoscopic model shown in Fig. 3 is available in 3-D so far, and allows a fly-through animation with inclusion of the CFD data as well as raw IVUS images [10]. Since the raw IVUS data is annotated with an opacity value and encoded into VRML, this scene resulted in 130 MB of automatically generated VRML code. CFD analysis was performed in all six phases. Maximum shear stress occured upstream (proximal) of the stenosis as expected. In accordance with previous validation in uniformly curved tubes [5], higher shear stress distributions along the vessel curvature were seen on the outer wall as compared to the inner wall. In unstenosed regions, τ values up to approximately 15 Pa were identified at the outer wall, whereas $\tau \leq 5.6$ Pa were identified on the inner wall. In the stenotic region, the shear-stress distribution showed τ values exceeding 100 Pa.

5. DISCUSSION

The observed shear stress distributions along the stenotic vessel segment selected for the feasibility study correspond to those reported in other studies. In-vitro validation of our CFD software was successful and the in-vivo application in multiple heart phases showed good performance. To obtain a complete 4-D analysis, the CFD software will have to be extended to consider pulsatile unsteady flow, and especially vessel movement during the heart cycle. It is expected that the results differ considerably as compared to the simple 3-D case, since the rapid movement of the epicardial surface, and thus the coronary arteries, substantially influences the flow conditions inside the vessel. Another topic addresses the correspondence of vertex points between phases; since segmentation and the determination of the absolute frame orientation are coupled in IVUS, and angiographic changes of the 3-D length of main vessel segments were shown to be below intraobserver variability [8], this correspondence seems to be stable. However, the catheter usually does not follow the vessel centerline, and therefore slight longitudinal displacements need to be accounted for. After the results are available, VRML visualization allows user-friendly manipulation of the scene and ensures platform-independence. While the external prototype library is small (47 KB) and shared between all scenes, the contour and IVUS pixel data may result in several megabytes of fully-automatically generated VRML code. Thus, respective computational and graphics hardware power is required. Our configurations using the *CosmoPlayer* 2.1 (CosmoSoftware, Computer Associates International Inc., Islandia NY, U.S.A.) with *Netscape* 4.7 on either SGI *Onyx* 2 (IRIX 6.5, 576 MB RAM) or *Pentium* III (NT 4.0/Win2000, 256/512 MB) machines showed excellent performance.

6. CONCLUSION

In this preliminary study, we have demonstrated the ability to reconstruct the morphologically realistic geometry of the coronary arteries from the fusion of IVUS and angiographic imaging modalities. We now have the ability of reconstruction of the coronary vessel geometry

as a function of time in order to delineate the motion of the artery during a cardiac cycle. The virtual angioscopy approach enables a better assessment of the reconstructed and calculated data in a local context, and can be used for didactical purposes as well. Our aim is to use CFD simulation and the computation of wall shear stress distribution in coronary vessels with the inclusion of the vessel distensibility as well as the translation and geometrical changes of the artery during a cardiac cycle in order to correlate the flow induced stresses with the development and growth of atherosclerotic lesions in these vessels.

ACKNOWLEDGMENTS

This work was supported in part by the *Deutsche Forschungsgemeinschaft*, Bonn, Germany (Wa 1280/1-1); and by the *National Institutes of Health*, Bethesda MD, U.S.A. (R01 HL63373).

REFERENCES

[1] J. H. C. Reiber, G. Koning, J. Dijkstra, A. Wahle, B. Goedhart, F. H. Sheehan, and M. Sonka. "Angiography and intravascular ultrasound," in *Handbook of Medical Imaging — Volume 2: Medical Image Processing and Analysis*, M. Sonka and J. M. Fitzpatrick (eds), pp. 711–808. SPIE Press, Bellingham WA, 2000.

[2] A. Wahle, G. P. M. Prause, S. C. DeJong, and M. Sonka. "Geometrically correct 3-D reconstruction of intravascular ultrasound images by fusion with biplane angiography — methods and validation," *IEEE Transactions on Medical Imaging*, vol. 18, no. 8, pp. 686–699, Aug. 1999.

[3] A. Wahle, G. P. M. Prause, C. von Birgelen, R. Erbel, and M. Sonka. "Fusion of angiography and intravascular ultrasound in-vivo: Establishing the absolute 3-D frame orientation," *IEEE Transactions on Biomedical Engineering — Biomedical Data Fusion*, vol. 46, no. 10, pp. 1176–1180, Oct. 1999.

[4] K. B. Chandran, M. J. Vonesh, A. Roy, S. Greenfield, B. Kane, R. Greene, and D. D. McPherson. "Computation of vascular flow dynamics from intravascular ultrasound images," *Medical Engineering and Physics*, vol. 18, no. 4, pp. 295–304, June 1996.

[5] A. Wahle, S. C. Mitchell, S. D. Ramaswamy, K. B. Chandran, and M. Sonka. "Four-dimensional coronary morphology and computational hemodynamics," in *Medical Imaging 2001: Image Processing*, M. Sonka and K. M. Hanson (eds), vol. 4322. SPIE Proceedings, Bellingham WA, Feb. 2001, (in press).

[6] C. M. Gibson, L. Diaz, K. Kandarpa, F. M. Sacks, R. C. Pasternak, T. Sandor, C. L. Feldman, and P. H. Stone. "Relation of vessel wall shear stress to atherosclerosis progression in human coronary arteries," *Arteriosclerosis and Thrombosis*, vol. 13, no. 2, pp. 310–315, Feb. 1993.

[7] S. L. Waters. *Coronary Artery Haemodynamics: Pulsatile Flow in a Tube of Time-Dependent Curvature*, Ph.D. Thesis, University of Leeds, United Kingdom, 1996.

[8] E. Wellnhofer, A. Wahle, I. Mugaragu, J. Gross, H. Oswald, and E. Fleck. "Validation of an accurate method for three-dimensional reconstruction and quantitative assessment of volumes, lengths and diameters of coronary vascular branches and segments from biplane angiographic projections," *International Journal of Cardiac Imaging*, vol. 15, no. 5, pp. 339–353, Oct. 1999.

[9] Y. G. Lai and A. J. Przekwas. "A finite-volume method for fluid flow simulations with moving boundaries," *Computational Fluid Dynamics*, vol. 2, pp. 19–40, 1994.

[10] A. Wahle, S. C. Mitchell, S. D. Ramaswamy, K. B. Chandran, and M. Sonka. "Virtual angioscopy in human coronary arteries with visualization of computational hemodynamics," in *Medical Imaging 2001: Physiology and Function from Multidimensional Images*, C. Chen and A. V. Clough (eds), vol. 4321. SPIE Proceedings, Bellingham WA, Feb. 2001, (in press).

[11] T. J. Pedley. *The Fluid Mechanics of Large Blood Vessels*. Cambridge University Press, Cambridge/New York, 1980.

[12] J. G. Myers, J. A. Moore, M. Ojha, K. W. Johnston, and C. R. Ethier. "Factors influencing blood flow patterns in the human right coronary artery," *Annals of Biomedical Engineering*, vol. 29, no. 2, pp. 109–120, Feb. 2001.